PROCEEDINGS OF SCIENCE

Advances in the simulation system of the ASTRI Project

F. G. Saturni,[a,b,*] **C. Bigongiari,**[a,b] **F. Casaburo,**[a,c,d] **L. A. Antonelli,**[a] **E. Fedorova,**[a] **G. Zacharis,**[a] **V. Giordano,**[e] **G. Leto,**[e] **C. Casentini,**[f] **T. Mineo,**[g] **D. Mollica**[g] **and S. Iovenitti**[h] **for the ASTRI Project**[i]

[a] *INAF – Osservatorio Astronomico di Roma, Via Frascati 33, I-00078 Monte Porzio Catone (RM), Italy*
[b] *ASI – Space Science Data Center, Via del Politecnico snc, I-00133 Roma, Italy*
[c] *INFN – Sezione di Roma 2, Via della Ricerca Scientifica 1, I-00133 Roma, Italy*
[d] *Università degli Studi di Roma "La Sapienza", P.le A. Moro 5, I-00185 Roma, Italy*
[e] *INAF – Osservatorio Astrofisico di Catania, Via S. Sofia 78, I-95123 Catania, Italy*
[f] *INAF – Istituto di Astrofisica e Planetologia Spaziali, Via del Fosso del Cavaliere 100, I-00133 Roma, Italy*
[g] *INAF – Istituto di Astrofisica Spaziale e Fisica Cosmica, Via U. La Malfa 153, I-90146 Palermo, Italy*
[h] *INAF – Osservatorio Astronomico di Brera, Via E. Bianchi 46, I-23807 Merate (MI), Italy*
[i] http://www.astri.inaf.it/en/library/
E-mail: francesco.saturni@inaf.it, ciro.bigongiari@inaf.it, fausto.casaburo@inaf.it

The ASTRI Mini-Array is an INAF project aimed at constructing an array of nine imaging air Cherenkov telescopes (IACTs) for the very-high energy γ-ray detection at the Teide Observatory site (Tenerife, Canary Islands), finalised to observe astronomical objects emitting photons in the multi-TeV spectral band. Detailed simulations of atmospheric showers of Cherenkov events using Monte-Carlo (MC) methods are needed to estimate the expected performance of the ASTRI Mini-Array and its precursors, such as the ASTRI-*Horn* prototype located at the Serra La Nave observing station (Mt. Etna, Sicily) and the ASTRI Mini-Array reduced configurations composed by less than nine telescopes. Such simulations are also needed to validate the MC simulation chain, for calibration purposes and for the development of ancillary instruments, and must be performed taking into account a variety of different hardware set-up and observing conditions. The production of events detected by IACTs is carried out with the `CoRSiKa` software and the `sim_telarray` package. In this contribution, we present the latest developments of the ASTRI Project simulation system in the framework of the commissioning of the first ASTRI Mini-Array telescope (ASTRI-1), describing in detail the software pipeline adopted for the generation of MC events, the hardware facilities dedicated to run the simulations and the final products delivered for higher-level analyses.

39th International Cosmic Ray Conference (ICRC2025)
15–24 July 2025
Geneva, Switzerland

ICRC 2025
The Astroparticle Physics Conference
Geneva July 15-24, 2025

*Speaker

PoS(ICRC2025)832

1. Introduction

The study of very-high energy (VHE) sources, harboring phenomena that emit photons of energy $E_\gamma > O(0.1\ \text{TeV})$ – γ-ray bursts, jets originating from active galactic nuclei, pulsars and supernova remnants, ionized winds in Seyfert and starburst galaxies, interaction of cosmic rays (CRs) and elusive processes expected from dark matter particles in galactic halos – is one of the main topics of the current and future γ-ray astronomy [1, 2]. Huge steps forward have been done in this field over the last years thanks to current ground-based instruments, in particular the imaging atmospheric Cherenkov telescopes (IACTs) like VERITAS [3], H.E.S.S. [4] and MAGIC [5]. The next-generation IACTs – especially the ASTRI Mini-Array [6, 7] and the first telescopes of the forthcoming Cherenkov Telescope Array Observatory (CTAO) [8] – will be of paramount importance to clarify the nature of the γ-ray emission from already detected sources and discover new ones, thanks to their unprecedented sensitivity and angular resolution [9, 10].

The ASTRI ("Astrofisica con Specchi a Tecnologia Replicante Italiana") Project was born as a flagship project of the Italian National Institute for Astrophysics (INAF) [11], aimed at developing an end-to-end CTAO pathfinder composed by several small-sized telescopes (SSTs) [12] in dual-mirror configuration. A first prototype, the ASTRI-*Horn* telescope [13], is currently operative at the INAF "M. C. Fracastoro" observing station in Serra La Nave (Mt. Etna, Italy). The further step of this project is the installation of the ASTRI Mini-Array, an array of nine ASTRI telescopes, at the *Observatorio del Teide* in Tenerife (Canary Islands, Spain). The first telescope (ASTRI-1) is currently taking data for both the system verification and the first scientific observations of astrophysical targets, and will be shortly followed by other three instruments (ASTRI-2, ASTRI-3 and ASTRI-4) to initiate stereoscopic acquisitions by the end of 2025. The complete ASTRI Mini-Array will be able to study in detail relatively bright sources ($E_\gamma^2 \times dF/dE_\gamma \sim 10^{-12}$ erg s^{-1} cm^{-2} at 10 TeV), with an angular resolution of ∼3 arcmin and an energy resolution of ∼10% at energies of ∼10 TeV that are affected by little degradation up to 100 TeV [14].

2. The ASTRI simulation system software chain

Beside the major efforts that are underway for the on-site deployment of the hardware components, the ASTRI Project team is working as well on the development of the software tools needed to pre-process, reduce and analyze the collected data. A consistent part of such software is included in the ASTRI Mini-Array simulation system, a collection of software components that are in charge of generating all of the Monte Carlo (MC) simulated data needed in all of the ASTRI Project phases. In particular, such MC simulations are used in the commissioning and operation phase of the instrument to:

- provide auxiliary inputs for the reconstruction of real Cherenkov events through the generation and application of suitable reconstruction models;
- obtain the response of the system to γ-ray astrophysical observations by means of the generation of appropriate instrument response functions (IRFs) [15].

The simulation of the Cherenkov events recorded by IACTs starts with the generation of the development of particle cascades in the atmosphere with the associated emission of Cherenkov

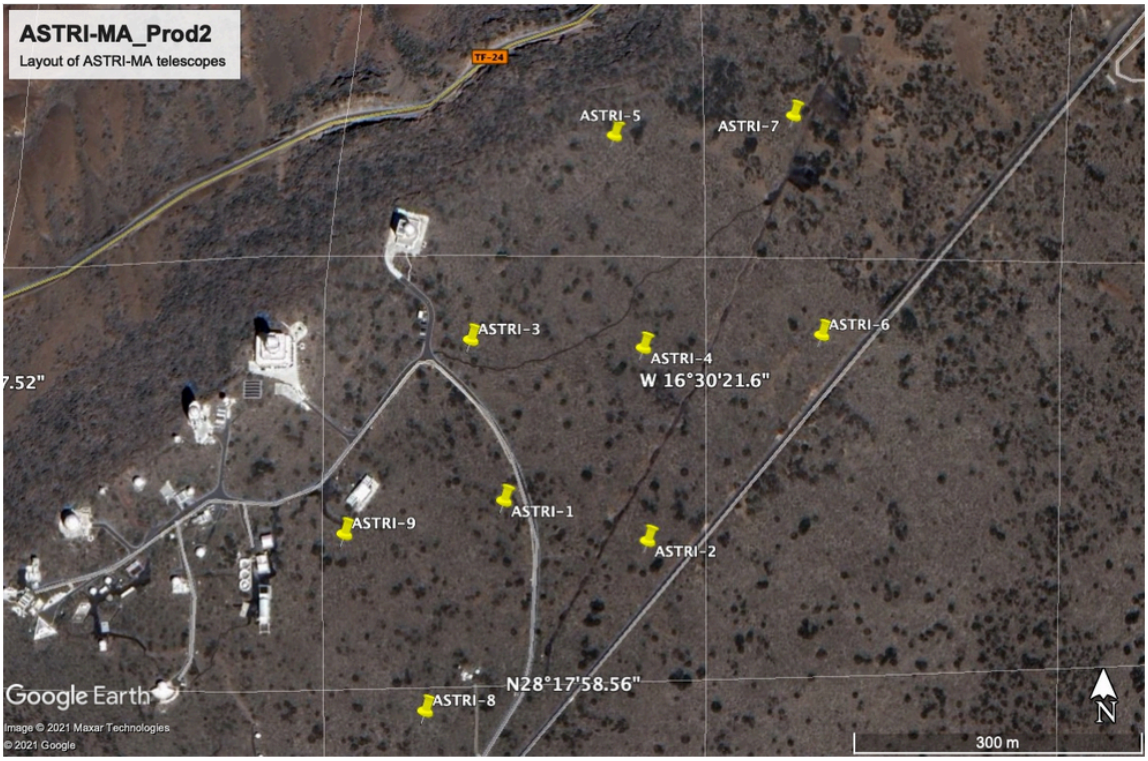

Figure 1: Layout of the ASTRI Mini-Array telescopes under construction at the *Observatorio del Teide* site.

light – a task carried out with the `CoRSiKa` software package[1], that performs detailed simulation of extensive air showers initiated by VHE CRs [16]. Such showers are tracked by `CoRSiKa` through the atmosphere until they undergo reactions with the air nuclei, generating Cherenkov radiation; this radiation is then converted to event images through the reproduction of the telescope and detector response to the impinging light – simulated with the `sim_telarray` software package [17], which can be flexibly configured at run-time depending on the telescope system.

Both steps of the simulation chain are usually very demanding in terms of computing power and disk space. Furthermore, since the Cherenkov imaging technique achieves a very high background rejection, huge numbers of hadronic events need to be simulated to properly estimate the instrumental performances. To cope with such requirements, massive productions of simulated events for the ASTRI Mini-Array commissioning and operation phases are being carried out through an extensive use of the ASTRI Data Center [18, 19] – a new facility for high-performance calculus located at the Astronomical Observatory of Rome (Italy) – and the resources of the *Pleiadi* cluster[2] – a computational infrastructure for science deployed at the Astronomical Observatory of Catania (Italy).

[1] Available at `https://www.iap.kit.edu/corsika/`.
[2] See `https://pleiadi.readthedocs.io/en/latest/index.html` for details.

Particle type	Spectral slope	Energy range (TeV)	View-cone radius (deg)	Scatter radius (m)	Azimuth (deg)	Zenith angle (deg)	No. of simulated showers
			ASTRI-MA Prod2_20deg				
Photons (point-like)	−1.5	0.1 – 330	0	3200	0/180	20	4×10^7
Photons (diffuse)	−1.5	0.1 – 330	10	3200	0/180	20	4×10^8
Electrons	−1.5	0.1 – 330	10	3200	0/180	20	2×10^8
Protons	−1.5	0.1 – 660	10	3200	0/180	20	2×10^9
Helium nuclei	−1.5	0.12 – 750	10	3200	0/180	20	1.2×10^8
			ASTRI-MA Prod2_40deg				
Photons (point-like)	−1.5	0.16 – 530	0	4000	90/270	40	4×10^7
Photons (diffuse)	−1.5	0.16 – 530	12	4000	90/270	40	4×10^8
Electrons	−1.5	0.16 – 530	12	4000	90/270	40	2×10^8
Protons	−1.5	0.16 – 1060	12	4000	90/270	40	2×10^9
Helium nuclei	−1.5	0.16 – 2120	12	4000	90/270	40	1.2×10^8
			ASTRI-MA Prod2_60deg				
Photons (point-like)	−1.5	0.5 – 800	0	6000	0/90/180/270	60	4×10^7
Photons (diffuse)	−1.5	0.5 – 800	14	6000	0/90/180/270	60	4×10^8
Electrons	−1.5	0.5 – 800	14	6000	0/90/180/270	60	2×10^8
Protons	−1.5	0.5 – 1600	14	6000	0/90/180/270	60	2×10^9
Helium nuclei	−1.5	0.5 – 3200	14	6000	0/90/180/270	60	1.2×10^8

Table 1: Main `CoRSiKa` parameters describing the MC air shower simulations generated so far in the framework of the ASTRI-MA Prod2 sub-productions for the ASTRI Mini-Array at the *Observatorio del Teide* site. For the helium nuclei at a zenith angle of 20°, the simulation parameters are slightly different with respect to those holding for the other particle due to their later addition to the MC production. For the same reason, only part of the total available statistics (∼67%) is being currently used in the analysis of the ASTRI-1 real data.

3. The updated ASTRI Mini-Array MC productions

In view of the construction of the ASTRI Mini-Array at the *Observatorio del Teide* site, we produced a massive `CoRSiKa` MC simulation – called "ASTRI-MA Prod2" – of γ-rays coming from point-like sources, along with diffuse γ-rays, electrons, protons and helium nuclei with incoming directions uniformly distributed in a cone of 10° radius centered on the point-like source direction. Contrary to the previous MC production – identified as "ASTRI-MA Prod1" [10, 20–22] – the current one takes into account the final positions of the ASTRI Mini-Array telescopes at the *Observatorio del Teide* site, officially approved by the end of 2020.

Since the performance of any IACT system significantly depends on the actual pointing directions, and the final layout of the ASTRI Mini-Array is quite elongated (see Fig. 1) – thus having an expected performance that shows non-trivial dependencies with respect to the azimuth (Az) pointing direction, particularly at medium and high zenith angles (ZAs) – the purpose of this MC production is:

1. to ensure a meaningful reduction and analysis of the real Cherenkov data collected with the first ASTRI telescopes (in particular ASTRI-1);

2. to characterize the ASTRI Mini-Array performance at different sets of ZAs and Az.

Parameter	Old value	New value	Units
Night-sky brightness (NSB) rate	0.122	0.060	GHz
Geometric offsets for reference point	N.A.	(30.5, 70.5)	cm
Primary mirror reflectivity	See Fig. 2	See Fig. 2	—
Secondary mirror reflectivity	See Fig. 2	See Fig. 2	—
Camera filter transmission	See Fig. 2	See Fig. 2	—
Random Gaussian fluctuations of the reflection angles	0.0255	0.05	deg
Angle-dependent off-axis transmission	(0.92362, 1, 0.03668, 1.7454, 0.858, 0.0)	(0.96, 1, 0.0368, 6.795, 0.45, 0.0)	—
Angle-dependent off-axis NSB profile	(1, 0.04478, 7.844, 2.0282)	(1, 0.92945, 50.91525, 2.62503, 7.18813)	—
Camera body diameter for shadowing	56.0	76.5	cm
Camera depth for shadowing	43.0	54.0	cm
Baffle around secondary mirror	(303.1, 281.9, 97, 10)	(294.8, 273.6, 97, 10)	cm
Diameter of secondary mirror shadowing	190.0	214.0	cm
Offset of secondary mirror shadowing	303.1	294.8	cm
Single photo-electron (SPE) response	See Fig. 3	See Fig. 3	—
Average photo-electron gain	4×10^4	3×10^6	—
Photo-detector transit time	1.0	0.5	ns
No. of pixel cells for pixel saturation	14400	8587	—
Photon detection efficiency (PDE) curve	See Fig. 3	See Fig. 3	—
No. of time bins for comparator simulations	85	160	—
No. of comparator time bins ahead of read-out	10	11	—
Comparator pulse shape	See Fig. 4	See Fig. 4	—
Signal amplification at comparator input	1.08696	1.037883	mV/p.e.
Comparator signal threshold per pixel	5.84	7.27	p.e.
Time over threshold for true logical response	1.5	6	ns
Effective comparator time slice length	8.0	3.333333	ns
Comparator output rise time	0.15	0.0	ns
Comparator output fall time	0.15	0.0	ns
Min. time of sector trigger over threshold	0.5	0.0	ns
Adjustment of trigger threshold	−0.5	0.0	—
No. of time bins to be filled	80	150	—
High-gain (HG) photo-electron equivalent (PEq)	28.953	97.90	ADC/p.e.
HG Gaussian white noise	0.52	26.06	ADC
Nominal HG pedestal value	2119.95	8446.5	ADC
Low-gain (LG) PEq	1.4477	4.90	ADC/p.e.
LG Gaussian white noise	0.1448	9.2	ADC
Nominal LG pedestal value	2128.1	8459.0	ADC
Data acquisition pulse shape	See Fig. 4	See Fig. 4	—
No. of time bins summed in ADC data	25	8	—
No. of time bins before trigger to start summing	−6	−4	—

Table 2: Relevant ASTRI Mini-Array parameters updated with respect to the configurations used for previous `sim_telarray` MC simulative production.

To this end, the telescope pointing was fixed at pre-determined combinations of ZAs and Az angles in a North-East-up (NEU) coordinate frame. Specifically, we simulated the directions $(\mathrm{ZA}, \mathrm{Az}) = (20°, 180°)$, $(40°, 90°)$ and $(40°, 270°)$ to reproduce the apparent trajectory of the Crab Nebula in the night sky during data-taking operations, together with the $(20°, 0°)$ direction to increase the event statistics at low ZAs. To ensure enough simulated event statistics in the highest energy bins (above several tens of TeV), we cast the energy of all primary particles according to a power-law energy spectrum with a spectral index equal to -1.5.

The three adopted ZA levels were organized into sub-productions called "ASTRI-MA Prod2_20 deg", "ASTRI-MA Prod2_40deg" and "ASTRI-MA Prod2_60deg", respectively. For each of them, we appropriately optimized the main `CoRSiKa` shower parameters as reported in Tab. 1. The first sub-production (ASTRI-MA Prod2_20deg) was launched in late 2020 and completed in early 2021; after that, the ASTRI-MA Prod2_60deg sub-production was fully generated by the second half of 2024. The last sub-production (ASTRI-MA Prod2_40deg) is currently underway, and will be completed by mid 2025.

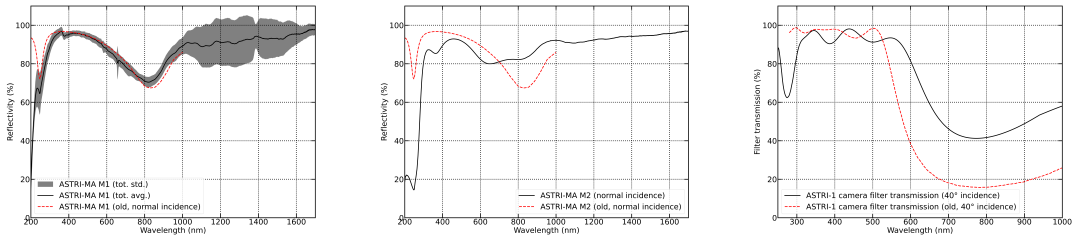

Figure 2: *Left panel:* average differential reflectivity of the ASTRI Mini-Array primary mirror (*black solid line*) as measured by the manufacturer, along with its uncertainty band at 68% confidence level (*grey band*). *Middle panel:* average differential reflectivity of the secondary mirror (*black solid line*). *Right panel:* differential transmission curve of the ASTRI-1 camera filter. In all plots, the synthetic curves computed from the mirror and filter coating chemical recipes (*red dashed lines*) – used in previous ASTRI Mini-Array MC simulation runs – are shown for comparison.

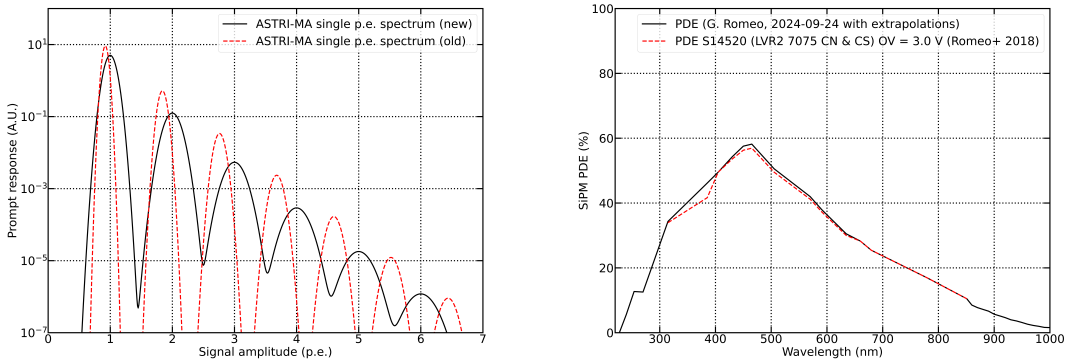

Figure 3: *Left panel:* updated SPE response of the ASTRI Mini-Array camera (*black solid line*), compared to the previously adopted one (*red dashed line*). *Right panel:* updated PDE of the ASTRI Mini-Array camera, (*black solid line*), compared to the one from [23] previously adopted in ASTRI MC simulations.

Then, we proceeded to update the ASTRI Mini-Array hardware parameters that are needed in input to `sim_telarray` to properly reproduce the instrument response to the `CoRSiKa` showers. To achieve this goal, we optimized – and in some cases remeasured – several telescope quantities that affect the `sim_telarray` internal ray tracing of the Cherenkov photons, the camera electronic response to the incident light, and the calculation of the background illumination. We report the main parameters updated in this way in Tab. 2. In Figs. 2, 3 and 4, we also show the comparisons between the previously adopted ASTRI Mini-Array performance curves and the updated ones.

In addition to the parameters described here, we are continuing the validation process of the simulation chain, which started in December 2018 with the real data taken with the ASTRI-*Horn* telescope [13] and is now being applied to ASTRI-1. Such a process requires many iterative comparisons between both calibration and scientific data acquired with the first camera(s) – first at a pixel level, and then at the image level for each available camera – and data simulated with different sets of input parameters, until a good match between the MC and real data is achieved at several analysis levels (pedestal widths due to background illumination, integral trigger rates, distributions

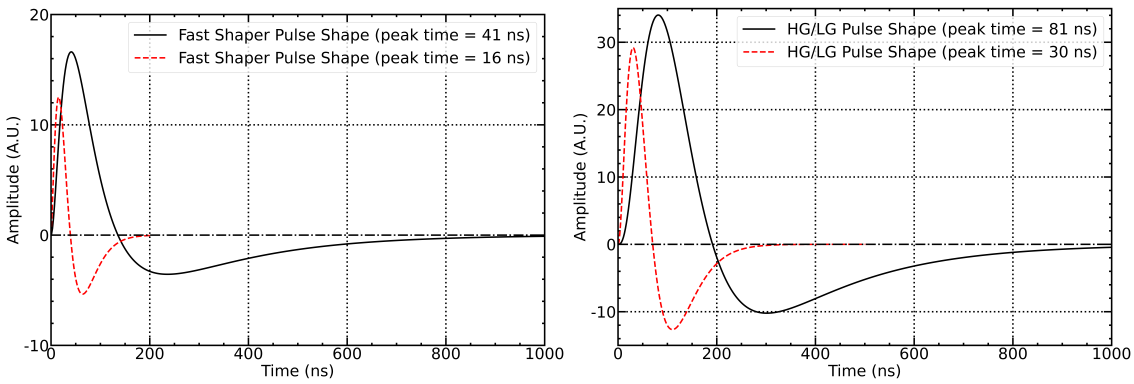

Figure 4: *Left panel:* updated comparator pulse shape (*black solid line*), along with the one previously adopted in the ASTRI Mini-Array MC simulations (*red dashed line*). *Right panel:* updated data acquisition pulse shape (*black solid line*), along with the one previously adopted in the ASTRI Mini-Array MC simulations (*red dashed line*). In both panels, the zero level (*black dot-dashed line*) is indicated.

of Hillas parameters used for energy reconstruction and gamma-hadron separation). As soon as at least two cameras will be installed, we will start to reconstruct events in stereoscopic mode and to perform comparisons at a higher level.

4. Updates to the ASTRI simulation plan

As described in Sect. 3, the updates to the ASTRI Mini-Array MC simulations have expanded the available datasets to observations of sources at ZAs in the interval $20° \div 60°$. This allows the data reduction and analysis of exposures of many scientifically interesting targets for the ASTRI Mini-Array, that can be observed from the *Observatorio del Teide* site only at medium-to-large ZAs. However, the NSB considered in the simulations has been set to dark conditions only – i.e. when the Moon is well below the horizon – so far. The possibility to extend the data-taking during weak and moderate Moon conditions is particularly important to increase the overall duty cycle of the system, as already shown for existing IACTs [25]: for these reasons, the full ASTRI-MA Prod2 will also cover different NSB levels [26].

In addition to the massive MC productions described above, we also need to simulate different types of events for calibration procedures and optimization of ancillary instruments and algorithms. Such ancillary simulations encompass the generation of:

- events for camera calibration (dark, laser and pedestal) needed to analyze the simulated events with the `A-SciSoft` software package [24], to provide (*i*) the complete reduction and analysis of the first scientific data acquired with ASTRI-1 and (*ii*) suitable IRFs for evaluating the system performance and carrying out scientific studies related to the ASTRI Mini-Array science program;

- muon-initiated events for the analysis of muon rings acquired by the ASTRI cameras, that are being used to estimate and monitor the overall optical throughput and optical point-spread function of the ASTRI telescopes;

- light emission by an illuminator that will serve as a cross-calibration device for the ASTRI telescopes.

The completion of a working stereo sub-array of four telescopes (ASTRI-1 to ASTRI-4; see Fig. 1) is planned by the end of 2025, with the subsequent start of scientific observations that will be used in turn for both the validation of the stereo data analysis chain and the delivery of the preliminary science products. In view of this step, further analyses of the MC simulated data generated in the framework of the ASTRI-MA Prod2 production are being planned to more carefully evaluate the system performances, such as the dependence of the energy threshold $E_{\rm thr}$ with the ZA [27] and the impact of the telescope throughput and pixel trigger multiplicity on the expected event trigger rate.

Acknowledgments

This work was conducted in the context of the ASTRI Project. We gratefully acknowledge support from the people, agencies, and organisations listed here: http://www.astri.inaf.it/en/library/. We acknowledge financial support from the ASI-INAF agreement no. 2022-14-HH.0. This paper went through the internal ASTRI review process.

References

[1] J. A. Hinton & W. Hofmann, ARA&A **47**, 523 (2009).
[2] A. De Angelis & M. Mallamaci, Eur. Phys. J. Plus **133**, 324 (2018).
[3] T. C. Weekes *et al.*, Astropart. Phys. **17**, 221 (2002).
[4] F. Aharonian *et al.*, A&A **457**, 899 (2006).
[5] J. Aleksić *et al.*, Astropart. Phys. **35**, 435 (2012).
[6] S. Scuderi *et al.*, JHEAP **35**, 52 (2022).
[7] A. Giuliani *et al.*, PoS **444**, 892 (2023).
[8] CTAO Cons., Astropart. Phys. **43**, 3 (2013).
[9] CTAO Cons., *Science with the Cherenkov Telescope Array*, World Scientific Pub. (2019).
[10] S. Vercellone *et al.*, JHEAP **35**, 1 (2022).
[11] G. Pareschi *et al.*, J. Phys. Conf. Ser. **718**, 052028 (2016).
[12] G. Tagliaferri *et al.*, Proc. SPIE **12182**, 121820K (2022).
[13] S. Lombardi *et al.*, A&A **634**, A22 (2020).
[14] S. Lombardi *et al.*, PoS **395**, 884 (2022).
[15] F. Pintore *et al.* PoS **444**, 722 (2023).
[16] D. Heck *et al.*, *CORSIKA: a Monte Carlo code to simulate extensive air showers*, TIB Hannover (1998).
[17] K. Bernlöhr, Astropart. Phys. **30**, 149 (2008).
[18] S. Lombardi *et al.*, PoS **444**, 682 (2023).
[19] M. Mastropietro *et al.*, PoS **444**, 765 (2023).
[20] F. G. Saturni *et al.*, JHEAP **35**, 91 (2022).
[21] A. D'Aì *et al.*, JHEAP **35**, 139 (2022).
[22] F. G. Saturni *et al.*, PoS **444**, 719 (2023).
[23] G. Romeo *et al.*, Nucl. Inst. Meth. Phys. Res. A **908**, 117 (2018).
[24] S. Lombardi *et al.*, Proc. SPIE **10707**, 107070R (2018).
[25] MAGIC Coll., Astropart. Phys. **94**, 29 (2017).
[26] F. G. Saturni *et al.*, PoS **444**, 717 (2023).
[27] MAGIC Coll., Astropart. Phys. **72**, 76 (2016).